

Groundwater Quality Assessment of Hassi Messaoud Region (Algerian Sahara)

Mahmoud Touahri¹, Mohamed Salah Belksier¹, Boualem Bouselsal^{1*}, Mokhtar Kebili²

¹ Laboratory of Underground Oil, Gas and Aquifer Reservoirs, Department of Earth and Universe Sciences, University of Kasdi Merbah, Route de Ghardaia, BP 511, 30000, Ouargla, Algeria

² Laboratory of Sedimentary Environment and Mineral and Water Resources in Eastern Algeria, Department of Earth Sciences, Larbi Tebessi University, Route de Constantine, 12002, Tébessa, Algeria

* Corresponding author's e-mail: bousboualem@gmail.com

ABSTRACT

In the Hassi Messaoud region, is groundwater the only source of water to meet daily demands, especially for consumption, domestic needs, industry and irrigation. This study focused on the evaluation of groundwater quality for potability and irrigation supply and the understanding of mineralization processes in the Mio-Pliocene (CTM), Senonian (CTS) and continental intercalary (CI) aquifers. For this study, 38 boreholes were sampled and analyzed for different parameters: pH, EC, TDS and major ions. The assessment of the relevance of groundwater in the study area was tested by the application of the water quality index (WQI) method. The suitability of the water for agricultural use was tested using the parameters of; EC, SAR, Na%, KR, PI and MH. The results illustrate that the groundwater in the study area is grouped into three classes: poor, very poor and unsuitable. Regarding groundwater use in irrigation, the results indicate that the waters of Hassi Messaoud are unsuitable for irrigation according on the EC and Wilcox diagram. The groundwater of the investigated area presents two types of water; Ca-Mg-HCO₃ and Ca-Mg-HCO₃. The study of the mineralization process of water using the Gibbs diagram and binary diagrams and the indices of saturation showed that the mineralization of water is controlled by the dissolution of evaporites and carbonates, silicate weathering and cation exchange. The participation of anthropic contributions is also noted in the Mio-Pliocene aquifer.

Keywords: Hassi Messaoud, CTM, CTS, CI, potability, irrigation, mineralization.

INTRODUCTION

The Hassi Messaoud region is of vital interest to the Algerian economy, as it is one of the ten largest hydrocarbon deposits in the world (Bouselsal 2017). Since the nineties, the region has experienced intense demographic development with increased industrial and agricultural activities. The arid climate and the absence of surface water resources in this region make the reliance on groundwater fatal. The fresh groundwater in the Hassi Messaoud region is stored in three aquifers: Continental Intercalary, Senonian and Mio-Pliocene (OSS 2010). Currently, the exploitation of these water reserves in the study area is of the order of 10 hm³/year for drinking water supply, 14 hm³/year for irrigation and 20.50 hm³/year for the petroleum

industry, of which 63.4% of the withdrawal are distinct to injection and workover operations.

In addition, the heavy exploitation of groundwater, the discharge of domestic and industrial wastewater, and the infiltration of irrigation water constitute negative effects on the groundwater quality. According to the recommendations of OSS (Sahara and Sahal Observatory) in 2003, it is necessary to control the chemical evolution of groundwater to ensure its sustainability and avoid a certain shortage in the region. To this end, the present study aimed to evaluate water quality for portability and irrigation and to improve the knowledge about the groundwater mineralization processes in the Hassi Messaoud region by interpreting hydrochemical data collected from existing water wells in the study area.

THE STUDY AREA

The study area is located in Hassi Messaoud (SE Algeria), bounded by longitude 31.6–31.8° North and latitude 5.9–6.2° East (Fig. 1). It covers an area of 820 km² and has a population of 55000 inhabitants (ONS 2021). A hyper-arid climate characterizes the study area. The metrological station reports reveal an average annual rainfall of about 34.6 mm and an average annual temperature of about 23.8°C (NOM 2021). From the geomorphological point of view, the area investigated is part of the Great Eastern Erg, characterized by a set of dunes, its altitude can reach 200 m.

GEOLOGY AND HYDROGEOLOGY SETTINGS

The geology of the study area is part of a set of structures forming North Eastern Triassic Province. It constituted the largest oil deposit in Algeria. The stratigraphic series of the area investigated is characterized by a gap of Paleozoic deposits resting on a granitic basement. Thus, the

Mesozoic deposits form an immense sedimentary series resting in discordance with the Paleozoic deposits (Cambro-Ordovician). The lower cretaceous is characterized by marine to continental facies changes between the Barrimian (clay, sandstone and dolomite), Aptian (crystalline dolomite) and Albian (sandstone, sand with silty clay). These formations constitute the continental intercalary reservoir complex. The upper cretaceous is represented from bottom to top by the Cenomanian formed by alternating anhydrite, marl and dolomite, constituting the impermeable roof of the continental intercalary aquifer. overlain by the Turonian consisting of limestone and the Senonian consisting of marl, anhydrite and rock salt at the base. On the other hand, the upper Senonian consists of limestone and dolomite. The geological formations of the upper Senonian constitute the Senonian aquifer (CTS), and the continental Tertiary, formed by sand, limestone and marl, corresponds to the Mio-Pliocene aquifer (CTM) (Cornet 1964; Busson 1967; Busson 1970; Castany 1982). The hydrogeological data interpretation shows that the aquifer system (Fig. 2) is composed of a superposition of the following

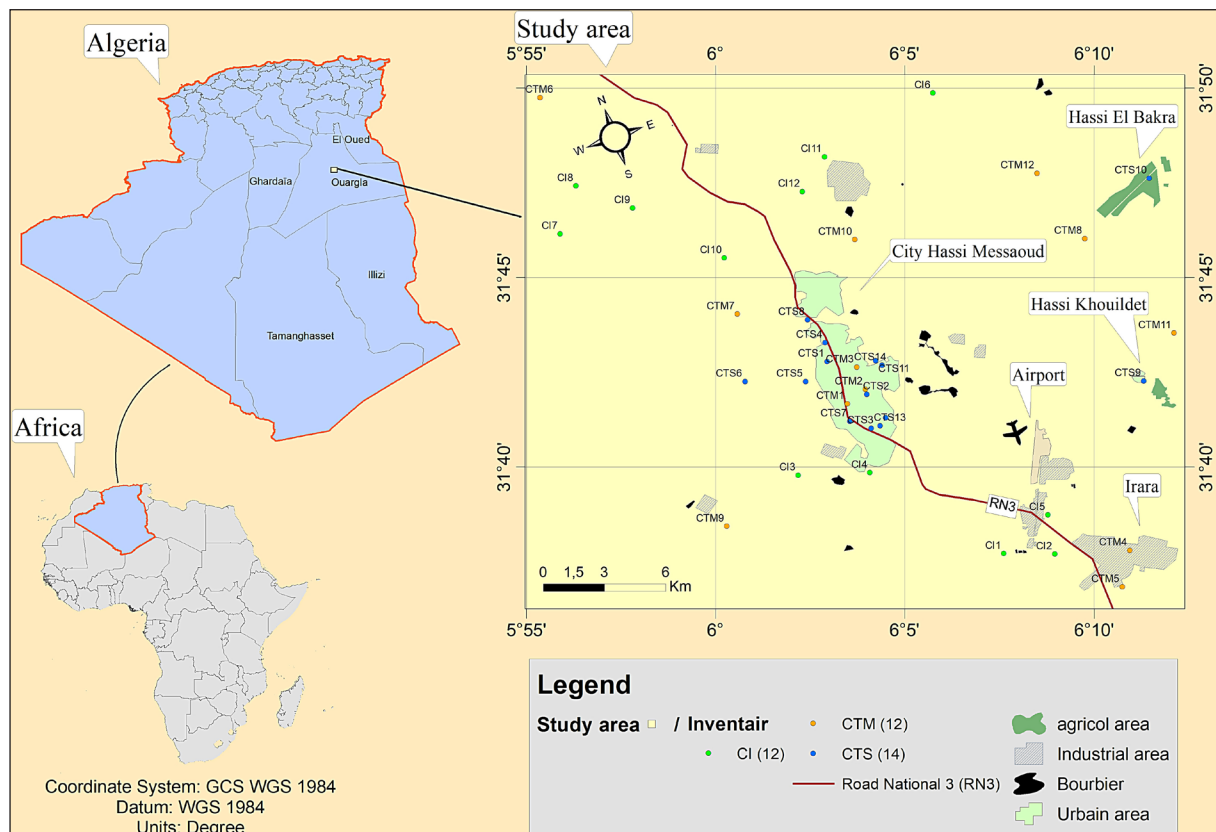


Figure 1. The area investigated of Hassi Messaoud region

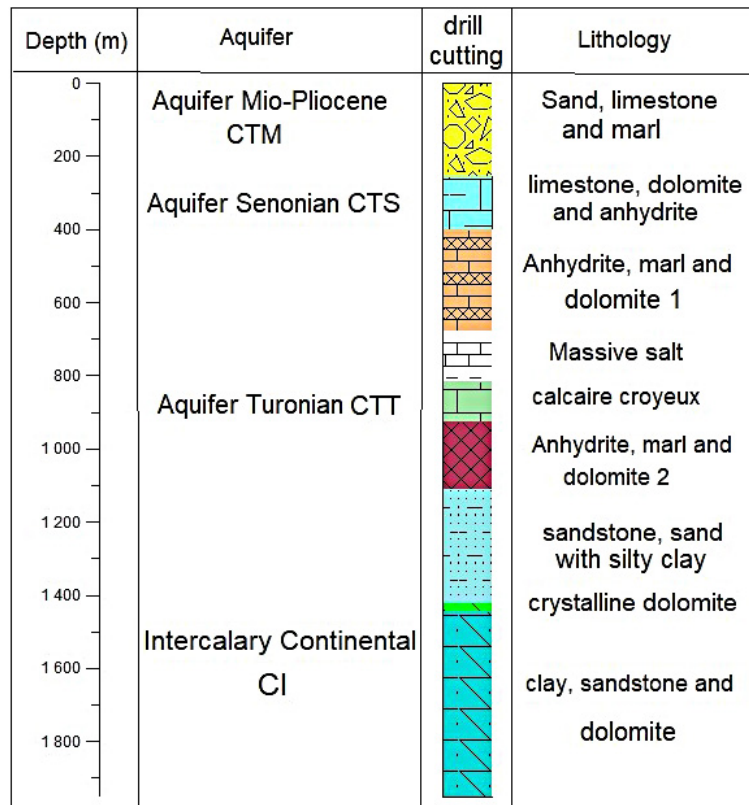


Figure 2. Log stratigraphy of water borehole in study area

aquifers (OSS 2010 ; UNESCO 1972 ; Satouh et al. 2021). The continental intercalary aquifer consists of sands and sandstones with some limestones and clay. Their depth is about 1150 m. The water pressure at the drilling head is about 15 bars, and the flow rate varies from one borehole to another. In abandoned oil boreholes converted into water boreholes, it oscillates between 30 and 60 l/s, but in ordinary water boreholes, it is about 100 l/s. The aquifer of complexe terminal (CT), groups two nappes; from top to bottom, it is distinguish (Bouselsal 2017) the aquifer of Mio-Pliocene consisting of sands with the presence of limestone and clay, their average thickness is 250 m, and the nappe of Senonian formed of dolomitic limestone and anhydrite, an approximate thickness of 150 m. The static level of the complexe terminal varies between 18 and 40 m, and the flow rate of the drillings varies between 15 and 30 l/s. The Turonian aquifer comprises dolomitic limestone, with an average thickness of 90 m. It is located at a depth of 800 m and separated from the two aquifer layers of the terminal complexe by a formation of the Senonian lagoon, which constitutes an impermeable screen. Although this aquifer is part of the terminal complexe, it is of no economic interest because of its very high salinity (210 g/l).

MATERIALS AND METHODS

A campaign of sampling and hydrochemical measurements was carried out in the area investigated. The 38 boreholes were selected to acquire data representative of the spatial variability of groundwater chemistry in Hassi Messaoud. The sampling points were distributed as follows: 12 boreholes tapping the Mio-Pliocene aquifer, 14 boreholes tapping the Senonian aquifer, and 12 boreholes tapping the continental intercalary aquifer. The physico-chemical parameters (pH and electrical conductivity) were measured in situ using a portable multiparameter. Samples were taken in polyethylene bottles after filtration for each water point.

The samples were analyzed in the laboratory of the technical production department (IRARA/EP) of Hassi Messaoud. The calcium, magnesium and chlorine were determined by titrimetry. Sulfate by photo-colorimetry, sodium and potassium using flame atomic absorption spectrometry. The ionic balance (IB) was calculated for the validity of the chemical analytical results of the waters. Thus, when the IB value obtained by formula 1 is $\leq 5\%$, the analytical results are considered valid, allowing further interpretation of the data.

$$IB = \frac{(|\sum \text{cations} - \sum \text{anions}|)}{(\sum \text{cations} + \sum \text{anions})} * 100 \quad (1)$$

Several computer programs were used in this study, namely SPSS version 26, for the statistical analysis of the chemical analysis results and the evaluation of the water quality, Diagrams 6.4 and AqQA 5.1 were prepared for the realization of the Piper, Chadha, Gibbs and bivariate diagrams, and to calculate the saturation indices. The evaluation of the potability of groundwater was carried out by using the method of water quality index (WQI). The relevance of water for irrigation was evaluated by studying the parameters that affect the soil and the plant (Arfa et al. 2022; Kebili et al. 2021): electrical conductivity (EC), sodium percentage (Na%), sodium, adsorption ratio (SAR), permeability index (PI), Kelly ratio (KR) and magnesium hazard (MH). These parameters were calculated using equations 2 to 6.

$$\text{Na \%} = \frac{(\text{Na} + \text{K}) \times 100}{\text{Na} + \text{K} + \text{Ca} + \text{Mg}} \quad (2)$$

$$\text{SAR} = \frac{\text{Na}}{\sqrt{\frac{\text{Ca} + \text{Mg}}{2}}} \quad (3)$$

$$\text{KR} = \frac{\text{Na}}{\text{Ca} + \text{Mg}} \quad (4)$$

$$\text{PI} = \frac{\text{Na} + \text{K} + \sqrt{\text{HCO}_3^-}}{\text{Ca} + \text{Mg} + \text{Na} + \text{K}} \times 100 \quad (5)$$

$$\text{MH} = \frac{\text{Mg}}{\text{Ca} + \text{Mg}} \times 100 \quad (6)$$

RESULTS AND DISCUSSIONS

Physico-chemical parameters of water

The results of the chemical analyses of the sampled water points are reported in Table 1. Electrical conductivity values range from 2022 to 3711 $\mu\text{s}/\text{cm}$, 2248 to 5969 $\mu\text{s}/\text{cm}$ and 2893 to 5528 $\mu\text{s}/\text{cm}$ for the CTM, CTS and CI aquifers, respectively. These groundwaters are classified as having very high salinity (Handa 1969). The concentration of total dissolved solids (TDS) in the groundwater varies between 1531 and 4326 mg/l (CTM), 1314 and 2586 mg/l (CTS) and 1947 and 2486 mg/l (CI). The measured values show that the groundwater of Hassi Messaoud is brackish water type (Freeze and Cherrey 1979). The pH values of the 3 aquifers in the area investigated vary between 7.6 and 7.8. Thus, these measured values are slightly alkaline and reflect a trend

towards neutrality. The total hardness (TH) values calculated for the three aquifers in the study area range from 530 to 2010 mg/l of CaCO_3 . According to Sawyer and McCarthy (1967), the ground water in the area investigated is very hard.

The calcium concentration ranges from 120 to 466 mg/l in the CTM aquifer, from 124 to 267 mg/l for the CTS aquifer and from 149 to 366 mg/l in the CI aquifer. The analyzed samples show that 75%, 35.71% and 50% of the CTM, CTS and CI waters, respectively, exceed the maximum allowable limit for drinking water (WHO 2017). The magnesium levels ranged from 22 to 366 mg/l (CTM), 85 to 150 mg/l (CTS) and 52 to 78 mg/l (CI). All the analyzed water samples from CTS and CI and 83.34% of the samples from CTM comply with the potability standard set by WHO (2017). The potassium in the groundwater of Hassi Messaoud varies between 11 and 90 mg/l. Only one sample (CTS8) was within the standard recommended by WHO (2017).

The chloride concentration ranges from 290 to 1337 mg/l for the TMC aquifer, from 155 to 678 mg/l in the CTS aquifer, and from 482 to 659 mg/l in the CI aquifer. The analyzed samples show that 83.33%, 42.85% and 91.66% of the waters of CTM, CTS and CI, respectively, exceed the maximum allowable limit for potassium water (500 mg/l). For sulfate, it varies from 400 to 1813 mg/l (CTM), 328 to 825 mg/l (CTS) and from 611 to 887 mg/l (CI). Except for water point CTS12, all analyzed water samples exceed the WHO (2017) standard of potability. The measured bicarbonate contents in the groundwater of the studied aquifers ranged from 106 to 323 mg/l. HCO_3^- originates from the dissolution of limestone and dolomite in the aquifer reservoirs.

The average nitrate concentration in CTM, CTS and CI varies at 32, 12 and 8 (Table 1). All the waters are within the norm of potability (50 mg/l). The high values measured in the miopliocene aquifer testify to the influence of anthropic factors on the chemistry of this aquifer. They are due to the infiltration of domestic water under urban areas and the return of irrigation water under agricultural land.

Water potability

The water potability assessment has been tested using the water quality index (WQI) method. This method measures various water quality parameters and then translates them cumulatively

Table 1. Chemical compositions of groundwater in the Hassi Messaud region

Parameter	Alg-Std (2011)	WHO 2017	CTM			CTS			CI		
			Min	Max	Mean	Min	Max	Mean	Min	Max	Mean
pH	6.5-8.5	6.5-8.5	7.05	7.83	7.6	7.63	7.85	7.70	7.1	7.8	7.5
CE	1500-2800	500-1500	2248	5969	4062	2022	3711	2765	2893	3528	3176
TH	100-500	100-500	530	2010	1071	700	1110	919	590	1200	788
TDS	1000-1500	500-1000	1531	4326	2752	1314	2586	1883	1947	2486	2168
Ca	100-200	75-200	120	466	248	124	267	193	149	360	213
Mg	50-150	50-150	22	366	110	85	150	106	52	78	63
Na	200	200	183	765	494	120	405	258	216	440	339
K	12	12	10	48	26	11	44	17	28	90	53
SO4	250-400	250-400	400	1813	917	328	825	656	611	887	719
Cl	250-500	250-500	290	1337	776	155	678	444	482	659	552
HCO ₃	-	300-500	106	251	149	124	293	198	180	323	219
NO ₃	50	45	10	50	32	5	16	12	4	15	8

into a single score. Therefore, the score produced is the integrated summary of scientific information from the water quality data in a format that is easily expressed and communicated to decision-makers and the public. Eq. 7 summarizes the steps required to calculate WQI (Brown et al. 1970; Vasanthavigar et al. 2010; Tiwari et al. 2017). This work considered the Algerian potability standards for calculating WQI (Table 2). The guide values (C_i), weights (w_p), and relative weights (W_p) of the chemical parameters were considered as given in the references of Bouselsal and Saibi (2022) and Ouarekh et al. (2021).

$$WQI = \sum \left[\left(\frac{w_p}{\sum_{i=1}^n w_p} \right) * \left(\frac{C_i}{S_c} * 100 \right) \right] \quad (7)$$

where: C_i – concentration of each parameter,
 S_c – Algerian standard values,
 w_p – the weight of each parameter,
 q_i – quality notation ($q_i = C_i/S_c$),
 W_p – the relative weight, ($W_p = w_p/\sum w_p$).

The WQI values were used to classify groundwater into five categories, namely, excellent, good, poor, very poor and undrinkable, as shown in Table 3. The calculated WQI values for groundwater in the study area ranged from 132 to 393, averaging 218. Three water quality classes were found (Fig. 3). The poor class represents about 71.4% of the water samples of the Senonian aquifer, 33.3% of the water samples of the Mio-Pliocene aquifer, and 33.3% of the water samples of the Continental Intercalary aquifer, the very poor class represents about 28.6% of the Senonian aquifer water samples, 25% of

Table 2. Weight of WQI parameters

Parameter	wp	S _c	Wp
pH	4	8.5	0.114
EC	4	1500	0.114
TDS	5	500	0.114
Ca	2	75	0.057
Mg	1	50	0.028
Na	2	200	0.057
K	2	12	0.057
Cl	3	250	0.085
HCO ₃	3	300 (WHO 2017)	0.085
SO ₄	4	250	0.114
NO ₃	5	50	0.114
Total	35	-	1

Table 3. Water quality index classification

Category	Index
Excellent	(<50)
Good	(50.1–100)
Poor	(100.1–200)
Very poor	(200.1–300)
Unsuitable for drinking	(>300.1)

the Mio-Pliocene aquifer water samples, and 66.7% of the Intercalary Continental aquifer water samples, and the undrinkable class represents about 41.7% of the Mio-Pliocene aquifer water samples. The high WQI values result from the high salinity of the groundwater in the study area. Groundwater salinization is mainly controlled by water-rock interaction. In addition, the infiltration

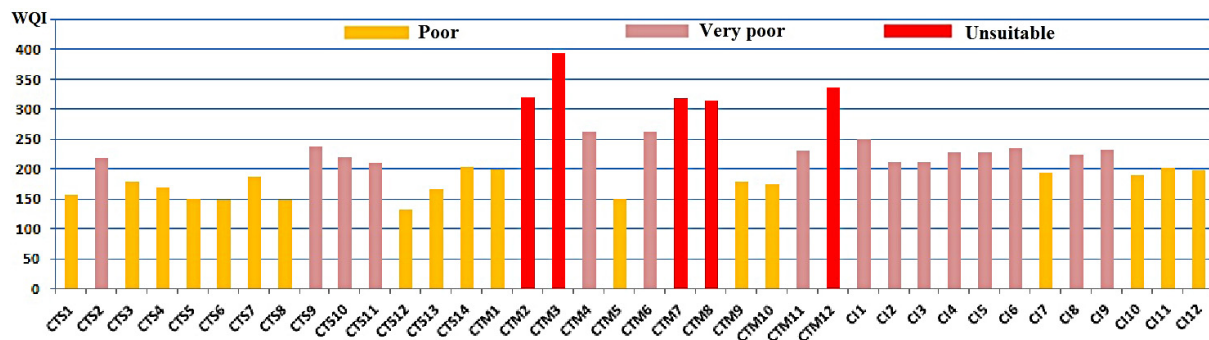


Figure 3. Water quality of groundwater in the Hassi Messaoud region

of surface water into the Mio-Pliocene aquifer has contributed to the degradation of the quality of the deep aquifers (CTS and CI).

Water quality for irrigation

Excessive mineral salts in water can have a detrimental impact on soil and plants. The salinity of irrigation water can disrupt plant development and reduce crop production. They also induce changes in the structure of the soil and make it impermeable to water and air. For these reasons, it is necessary to study the parameters of irrigation waters, such as EC, Na%, SAR, PI, KR and MH. The suitability of the waters for agricultural use was determined from comparison with the guide values determined by the following authors: Wilcox 1955 (EC), Richards 1954 (SAR), Wilcox 1948 (Na%), Doneen 1964 (PI) and Ragnunath 1987 (MH). The term “electrical conductivity” is synonymous with “specific electrical conductance”. The EC is expressed in $\mu\text{S}/\text{cm}$ and is generally used to indicate the total concentration of ionized constituents in natural water. It correlates well with the TDS value. Salinity increases the osmotic pressure of the soil water, which reduces water uptake by crop roots and leads to physiological drought. According to the threshold values established by Wilcox (1955), there are four classes of conductivity. The following can be distinguished: suitable for all types of crops and all kinds of soils when the conductivity $>250 \mu\text{S}/\text{cm}$ can be used, if a moderate amount of leaching occurs, normal salt-tolerant plants can be grown without much salinity control when conductivity varies between 250 and $750 \mu\text{S}/\text{cm}$, unsuitable for soil with restricted drainage when conductivity varies between 750 and $2250 \mu\text{S}/\text{cm}$, and unsuitable for soil irrigation when conductivity $> 2250 \mu\text{S}/\text{cm}$. The results of the hydrochemical measurements

carried out on the water samples showed that the waters of the Hassi Messaoud aquifers present EC oscillating between 2022 and $3711 \mu\text{S}/\text{cm}$ (CTM), 2248 and $5969 \mu\text{S}/\text{cm}$ (CTS) and from 2893 to $5528 \mu\text{S}/\text{cm}$ (CI). Four water samples from the Senonian aquifer (CTS5, CTS6, CTS8 and CTS12) belong to the class unsuitable for soil with restricted drainage. The other samples belong to the class unsuitable for soil irrigation.

Na% is an important parameter in the evaluation of groundwater for agricultural use. Equation 2 is used to calculate this parameter. Sodium influences the physicochemical properties of the soil and can also significantly affect the infiltration processes by reducing the permeability of the soil (Kharroubi et al. 2022). When the concentration of Na^+ is very high, the soil becomes compact and hard. This changes the structure of the soil and leads to the reduction of the air and water content in the soil. The values calculated in the study area vary between 8% and 22%. In reference to the classification of Wilcox (1948), the groundwater in the area is excellent for irrigation. The risk related to Na^+ is also determined by calculating the sodium adsorption ratio. Equation 3 is used to calculate this parameter. The SAR plays an important role in the evaluation of irrigation water because the amount of sodium allocated in the soil after absorption reduces the permeability of the soil and affects its structure. According to the classification established by Richards (1954), the waters of the investigated area are classified in the category excellent for irrigation, except for the point CTM10, classified in the category good for irrigation.

The SAR and EC values were plotted in the USSS diagram (1954). This diagram distinguishes 16 different categories of irrigation water in terms of sodium hazard and salinity hazard (Fig. 4a). The EC values indicate the salinity hazard on the X-axis (from low to very high), and the SAR

values indicate the alkalinity hazard on the Y-axis (from low to very high). Approximately 28.6% of the Senonian aquifer groundwater samples represent the C_3S_1 category, indicating high salinity and low sodium risks. Approximately 21.4% of the Senonian aquifer water samples, 8.3% of the Mio-Pliocene aquifer water samples and 8.3% of the Continental Intercalary aquifer water samples represent the C_4S_1 category, indicating high salinity risk and low sodium risk. Approximately 50% of the CTS aquifer water samples, 83.3% of the CTM water samples, and 41.6% of the CI water samples represent the C_4S_2 category, indicating high salinity risk and medium sodium risk. Finally, the C_4S_3 category, indicating high salinity risk and medium sodium risk, is represented by about 8.3% of the water samples from the Mio-Pliocene aquifer and 50% of the water samples from the Intercalary Continental aquifer. The combination of Na% and EC plotted on the Wilcox (1955) diagram (Fig. 4b) indicates that 25% of CTM, 64.3% of CTS and 16.7% of CI are in the poor class. The remaining samples (75% CTM, 35.7% CTS and 83.3% CI) belong to the poor class.

Kelly ratio (KR) is an important factor in assessing irrigation water quality. The equation 4 is used to calculate this parameter. KR less than 1 is considered suitable for irrigation, a Kelly ratio oscillating between 1 and 2 is considered unsuitable for irrigation and KR better than 2 is considered unsuitable for irrigation as it can seriously affect the permeability of the soil. The values found in the groundwater of the study area (Table 4) oscillated between 0.30 and 1.80, with an average of 0.87. According to the KR values obtained, the

water samples of the area investigated are shared between two classes; 50% of the CTM waters, 100% of the CTS waters and 41.7% of the CI waters in the class suitable for irrigation and 50% of the CTM waters and 58.3% of the CI waters in the class not suitable for irrigation (Table 4).

Soil permeability is important, because it allows groundwater to infiltrate the soil. The equation 5 is used to calculate this parameter. According to (Doneen, 1964), PI values are classified into Class 1 excellent, Class 2 good and Class 3 poor. According to Doneen (1964) and the calculation results shown in Table 5, the groundwater in the study area with a PI varies between 31% and 68%, with an average of 50%. They are therefore classified as good for irrigation with a maximum of 75% permeability. The magnesium risk is an essential parameter in assessing the irrigation water quality. The equation 6, developed by Raghunath (1987), calculates this parameter. According to Raghunath (198), MH values are classified into two classes: $MH < 50$ is considered suitable for irrigation and $MH > 50$ is unsuitable for irrigation, decreasing plant yields because the soil becomes more alkaline. In the present study, most of the water samples have MH values higher than 50% (Table 4), except for some points like (CTS3, CTS11, CTS12, CTS13, CTS14, CTM3 and CTM4).

Water type

The graphical presentation of major ions, cations and anions dissolved in the groundwater of the study area allows understanding their evolution and their hydrochemical distribution in

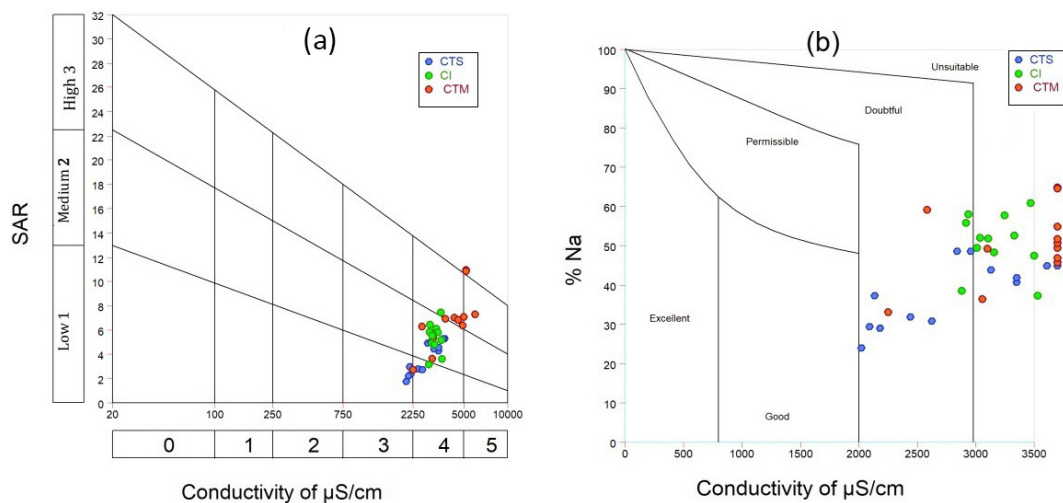


Figure 4. Diagrams of (a) US Salinity Laboratory (USSL) and (b) Wilcox

Table 4. Parmetres of groundwater quality

Sample	WQI	SAR	Na%	PI	KR	MH
CTS1	156	2.76	31.99	39.55	0.48	42.09
CTS2	218	4.33	39.45	45.79	0.67	40.94
CTS3	180	4.94	47.26	53.86	0.92	54.10
CTS4	168	2.80	30.76	38.32	0.45	47.43
CTS5	151	2.36	27.91	35.26	0.39	49.34
CTS6	149	2.26	28.02	37.17	0.40	45.63
CTS7	187	5.02	47.25	54.70	0.92	48.09
CTS8	149	1.77	22.82	31.68	0.30	46.90
CTS9	237	5.29	43.83	49.75	0.79	40.03
CTS10	220	5.29	43.83	47.84	0.79	40.03
CTS11	209	4.41	40.50	46.47	0.72	51.96
CTS12	132	2.96	35.05	42.40	0.56	55.84
CTS13	167	2.73	29.59	36.06	0.43	60.74
CTS14	204	4.59	40.27	45.26	0.69	50.13
CTM1	200	3.64	35.22	41.02	0.55	45.73
CTM2	319	7.10	47.87	51.63	0.95	43.52
CTM3	393	7.34	44.49	47.60	0.82	75.12
CTM4	263	7.05	50.19	53.56	1.02	74.99
CTM5	150	2.76	31.99	38.33	0.48	42.09
CTM6	263	6.88	50.20	53.96	1.04	44.80
CTM7	319	10.96	63.29	68.23	1.80	37.88
CTM8	313	10.89	63.04	67.97	1.78	37.95
CTM9	178	5.36	47.84	52.98	0.94	33.08
CTM10	175	6.32	56.37	63.53	1.38	39.20
CTM11	230	6.95	53.10	57.61	1.18	35.79
CTM12	337	6.39	44.68	48.67	0.84	19.41
CI1	250	3.61	32.71	39.15	0.52	25.33
CI2	212	4.93	44.53	53.56	0.88	29.30
CI3	212	3.16	32.71	41.72	0.53	32.18
CI4	229	4.80	42.81	52.74	0.83	31.28
CI5	227	7.47	56.98	65.02	1.46	36.29
CI6	234	6.11	50.33	60.47	1.19	32.53
CI7	194	5.85	51.83	60.35	1.17	35.77
CI8	224	5.80	48.78	56.91	1.03	37.27
CI9	232	5.18	43.85	50.83	0.83	33.28
CI10	188	6.43	55.44	63.82	1.32	37.42
CI11	201	5.56	49.21	56.51	1.02	35.01
CI12	198	5.52	49.26	56.76	1.03	34.14

space. For this purpose, the Piper and Chadha diagrams are used. The Piper's diagram (1944) (Fig. 5a) shows the cationic and anionic proportions on two equilateral triangles at the bottom combined on a diamond at the top, which traces all the major and minor elements dissolved in the groundwater. The Piper diagram clearly shows that 100% of the CI waters, 66.67% of the CTM waters and

85.74% of the CTS waters belong to the Ca-Mg-SO₄-Cl water types. The remaining 33.33% of the CTM water and 15.26% of the CTS water belong to the Ca-Mg-HCO₃ water type. The groundwater types in the study area were also identified by using Chadha's (1999) diagram (Fig. 5b). In this study, 83.33% of the groundwater samples of CI and CTM and 42.86% of the water of the CTS

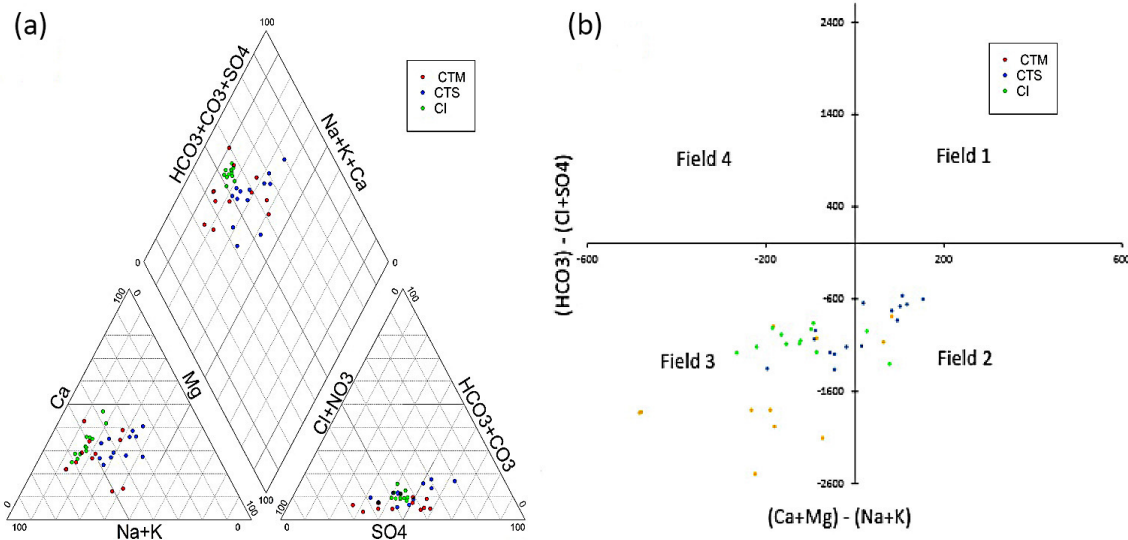


Figure 5. Piper (a) and Chadha (b) diagrams for the groundwater in study area

aquifer belong to field 3 (Na-Cl-SO₄). This means that these water samples are more alkaline (Na⁺ and K⁺) and strong acids (Cl⁻ and SO₄²⁻) than alkaline earth (Ca²⁺ and Mg²⁺) and weak acids (HCO₃⁻ and CO₃²⁻). This type of water develops salinity problems in drinking water. On the other hand, 57.14% of the CTS groundwater and 16.67% of the CI and CTS aquifer waters belong to field 2 (Ca-Mg-Cl-SO₄). This means these water samples are marked by more alkaline earth and strong acids than alkalis and weak acids. Furthermore, this water facies shows a mixture between the (Ca-SO₄) facies on the one hand and the reverse ion exchange on the other.

Geochemical processes

The geochemical study is the main method to determine the origin of dissolved ions in groundwater. For this purpose, the Gibbs diagram, the bivariate diagrams and the saturation index diagram were used. The Gibbs diagram (1970) is used to identify the origin of the salinity of groundwater. In this diagram of two equilateral parts, the first is the ratio Na/(Na+Ca) for cations, and the second is the ratio Cl/(Cl+HCO₃) for anions. The water samples are plotted separately against the respective TDS (in mg/l). The Gibbs diagram shows three domains defining the origin of the waters; the first domain represents the waters affected by the evaporation phenomenon, the second domain shows the waters resulting from the water-rock interaction, and the third domain defines the waters influenced by the precipitation phenomenon.

The Gibbs diagram (Fig. 6) illustrates that most of the groundwater of the investigated area result from evaporation processes more than the alteration of water-rock interaction.

The water-rock interaction can be summarized by three mechanisms: silicate alteration, carbonate formation, and evaporite dissolution. The origin of mineralization from water-rock interaction was determined by the mixing diagrams of Na normalized by Ca versus Na normalized by HCO₃ and Na normalized by Ca versus Na normalized by Mg (Fig. 7), first proposed by Gaillardet et al. (1999). Indeed, all the groundwater echoes in the study area fall between silicate alteration and evaporite dissolution domains.

In general, the content of dissolved ions in groundwater is controlled by the lithological nature of the aquifer (Schoeller 1962), the groundwater flow, the residence time of the water in the aquifer and the anthropogenic inputs into the free aquifer. The study of the correlations established between anions and cations allowed deducing the origin of the mineralization of waters. The strong positive correlation between these ions indicates the presence of a common source of salinity (Appelo and Postma 2005). For this study, mineralization origin was determined by using binary diagrams (Fig. 8).

The Na⁺ vs. Cl⁻ diagram (Fig. 8a) shows that Na and Cl ions are found near the 1:1 line for the CTS and CI water samples, which indicates that these ions come from the dissolution of the same source, the Halite (Bouselsal and Saibi, 2022). On the other hand, the CTM samples are dispersed by

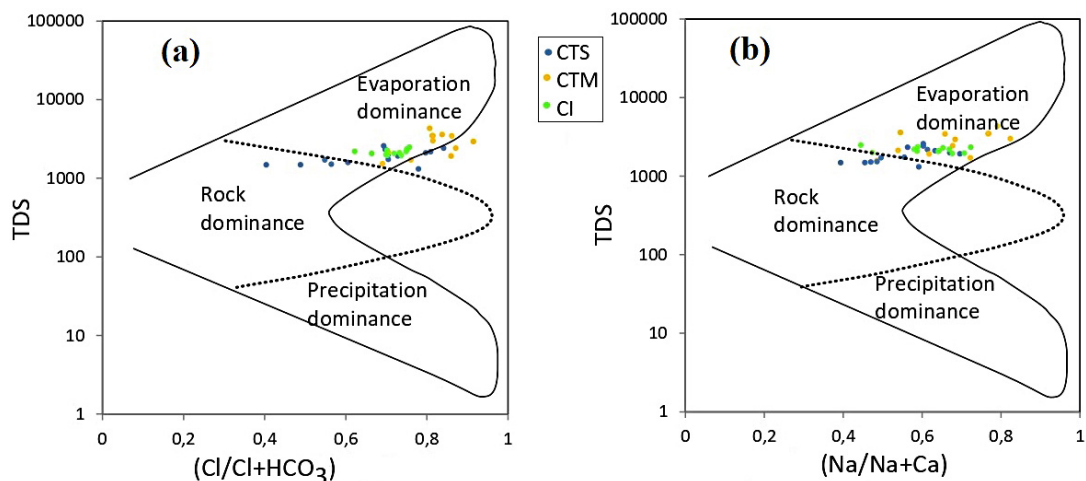


Figure 6. Gibbs diagram showing mechanisms controlling the water mineralization

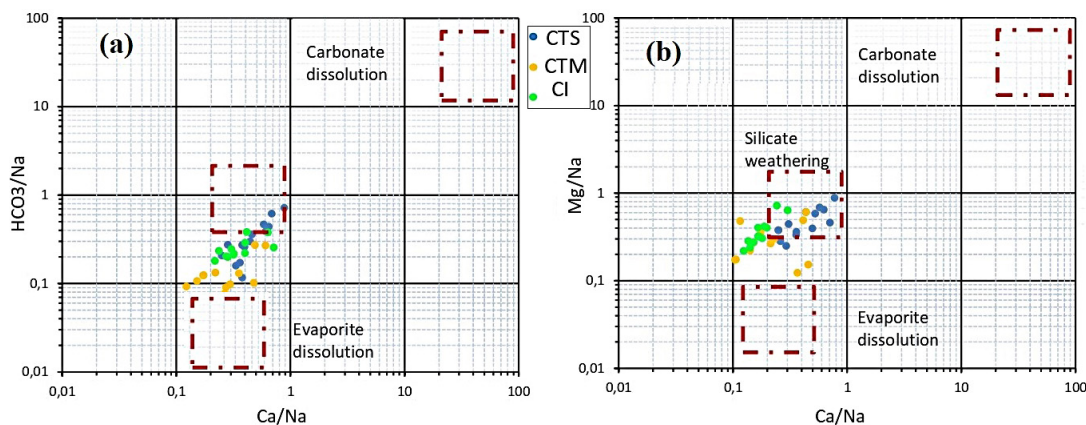


Figure 7. Relationships between (a) Ca/Na vs. HCO₃/Na, (b) Ca/Na vs. Mg/Na

the 1:1 line, which is explained by the existence of another origin of these ions, like the alteration of silicates, the cationic exchange and the anthropic contribution. The Ca²⁺ vs. SO₄⁻² diagram (Fig. 8b) shows a proportional evolution of Ca²⁺ and SO₄⁻² in the groundwater of CTS and CI, indicating the contribution of gypsum dissolution in the mineralization of the waters of these aquifers (Jia et al. 2020; Wisitthammasri et al. 2020). However, most of the samples are dissolved in the 1:1 line, indicating that the concentration of SO₄ is higher than that of Ca. This is explained by the existence of another origin of these ions, as previously indicated. The diagram (Ca²⁺ + Mg²⁺) versus (HCO₃⁻ + SO₄⁻²) (Fig. 8c) illustrates the participation of silicate alteration, carbonate dissolution and cation exchange in water mineralization (Tziritis et al. 2017). 41.6% of the CTM points, 78.5% of the CTS points and 25% of the CI points above the 1:1 line indicate the participation of carbonate and/or sulfate dissolution and/or reverse cation

exchange in water mineralization. The remaining points are influenced by silicate alteration. The diagram (Mg²⁺ + Ca²⁺) – (SO₄⁻² + HCO₃⁻) (Fig. 8d) was used to indicate the participation of cation exchange in the mineralization process of groundwater in the area investigated (Bouselsal and Zouari, 2022; Qu et al. 2020). Figure 8d indicates that 21% of the CTS points and 50% of the CTM waters exchange Na⁺ and K⁺ ions with Mg²⁺ + Ca²⁺ ions from the reservoir. In contrast, all sampled CI water points, about 25% of CTM water points, and 35% of CTS water points exchanged Mg²⁺ + Ca²⁺ ions with Na⁺ and K⁺ reservoir ions. The remaining sampled water points are near the (0,0) point indicating the absence of the cation exchange phenomenon.

Figure 9 shows the curves of the saturation indices of the main minerals established by the FREEQC software. In addition, Figure 8 shows that the CTM, CTS and CI groundwaters are characterized by an under-saturated state for the

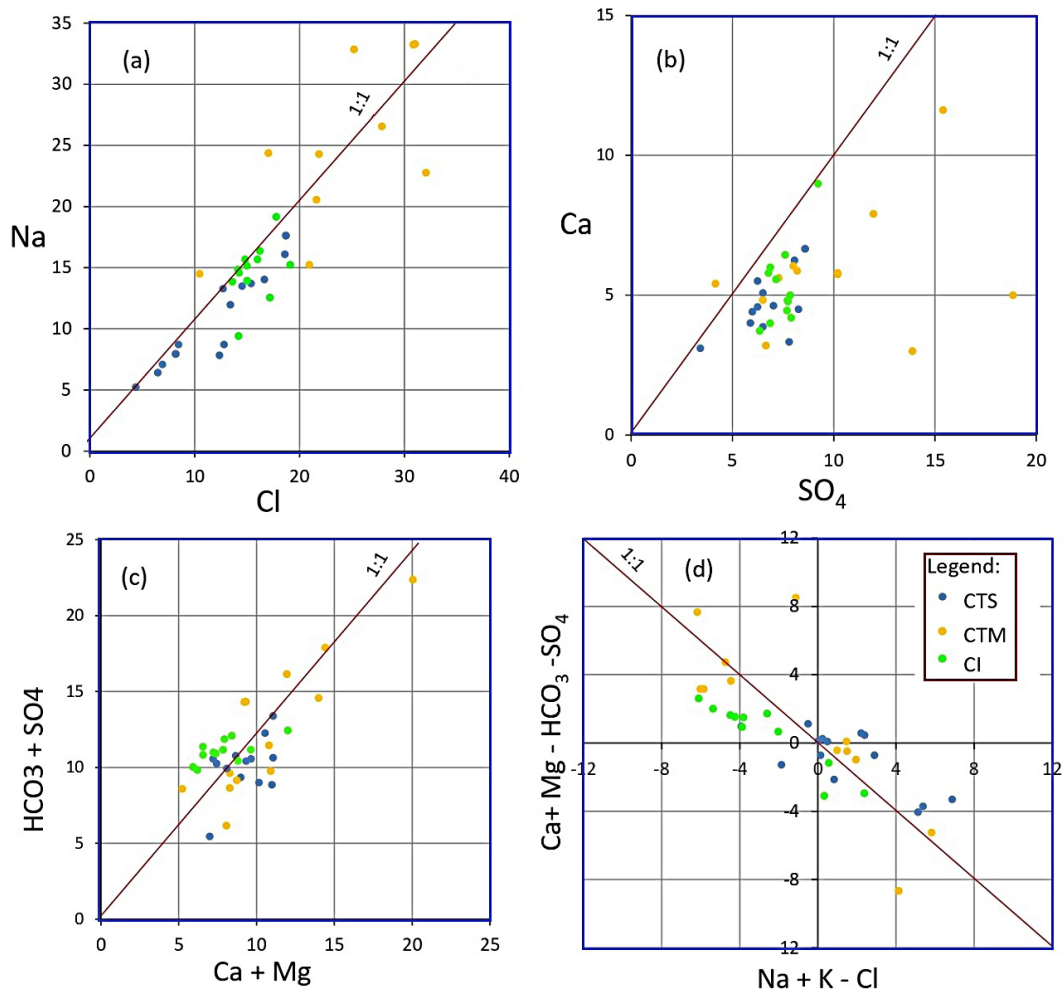


Figure 8. Binary diagrams between (a) Na vs. Ca, (b) SO₄ vs. Ca, (c) HCO₃+SO₄ vs. Ca+Mg, (d) (Mg + Ca) – (SO₄ + HCO₃) vs. (Na +K -Cl)

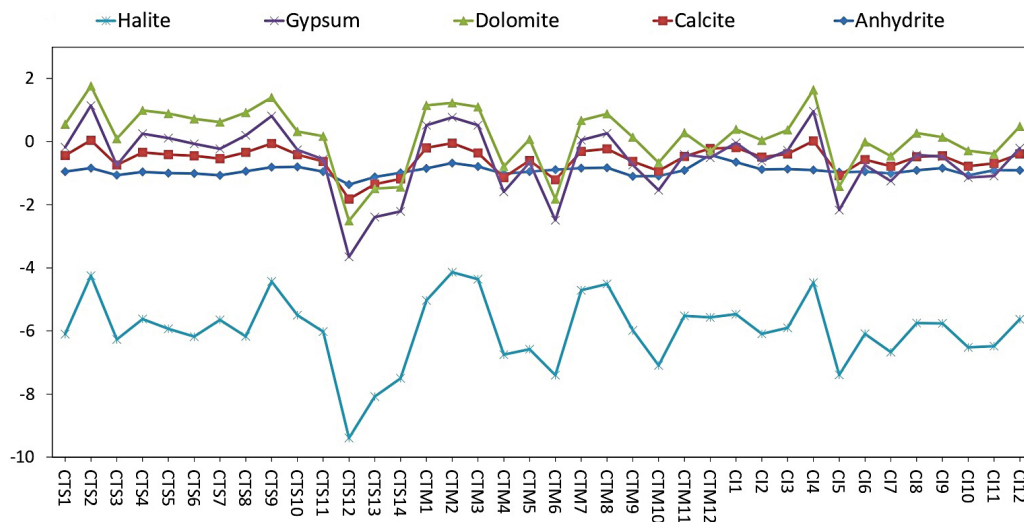


Figure 9. Mineral equilibrium diagram of groundwater of Hassi Massaud region

evaporite minerals (Halite, Anhydrite and Gyps), while a saturated state of the carbonic minerals (Calcite and Dolomite) is clearly visible for most

of the analyzed samples. This situation is compatible with the hydrochemical facies already described previously.

CONCLUSIONS

The Hassi Messaoud region is controlled by a hyper-arid climate where groundwater is the only source of water supply for different uses. This study evaluated the quality of water for human consumption and irrigation and the determination of the mineralization processes of groundwater. For this purpose, 38 boreholes sampled were taken from the three aquifers (CTM, CTS and CI) and analyzed. The relevance of the groundwater in the study region was evaluated by application the water quality index method. The relevance of the water for agricultural use was tested using the parameters of; electrical conductivity, sodium adsorption ratio, sodium percentage, Kelly ratio, permeability index and magnesium hazard. The results found that the groundwaters of Hassi Messaoud are grouped into three classes. The poor class represents about 71.4% of the water samples of the Senonian aquifer, 33.3% of the water samples of the Mio-Pliocene aquifer and 33.3% of the Continental Intercalary aquifer. The very poor class represents about 28.6% of the water samples of the Senonian aquifer, 25% of the water samples of the Mio-Pliocene aquifer and 66.7% of the Continental Intercalary aquifer. Moreover, the non-potable class represents about 41.7% of the water samples of the Mio-Pliocene aquifer. These results revealed that the waters of Hassi Messaoud require treatment before distribution.

For agricultural use, groundwater in the study area is classified as EC (unsuitable for soil with restricted drainage (10.5%) and unsuitable for soil irrigation (89.5%)), Na% (excellent for irrigation (100%)), SAR (excellent (97.4%), good (2.6%) and inappropriate (8%)), Kelly ratio (adapted (50% of CTM, 100% of CTS and 41.7% of CI) and unsuitable (50% of CTM and 58.3%)), PI (good (100%)) and MH (acceptable (81.2%) and not acceptable (18.4%)) In addition, the projection on the Wilcox diagram give that the water in the area investigated is in the poor or bad class for irrigation. The results revealed that the waters of Hassi Messaoud are unsuitable for irrigation, according to EC and the Wilcox diagram. The graphical presentation of the anions and cations of the groundwater of the area investigated on the Piper and Chadha diagrams reveals that 100% of the CI waters, 66.67% of the CTM waters and 85.74% of the CTS waters are of Ca-Mg-SO₄-Cl type, and 33.33% of the CTM waters and 15.26% of the CTS waters are of Ca-Mg-HCO₃ type. The

dominance of strong acids (Cl⁻ and SO₄²⁻) over weak acids (HCO₃⁻ and CO₃²⁻) is also observed. The study of water mineralization processes by the use of Gibbs diagrams and binary diagrams, as well as the saturation indices of the main minerals, allowed showing that the mineralization of waters results from the dissolution of evaporites (gypsum and halite) and carbonates (limestone and dolomite), silicate weathering and cation exchange. The participation of anthropic contributions is also noted in the Mio-Pliocene aquifer.

REFERENCES

1. Appelo C.A.J., Postma D. 2005. *Geochemistry, Groundwater and Pollution*. 2nd edition. CRC Press, New York.
2. Arfa A., Bouselsal B., Zeddouri A., Kebili M. 2022. Groundwater Geochemical and Quality of the Continental Intercalary Aquifer in Béni Ounif (Southwest Algeria). *Journal of Ecological Engineering* 2022, 23(9), 1–12. DOI: 10.12911/22998993/151070
3. Bouselsal B. 2017. Groundwater Quality in Arid Regions: The Case of Hassi Messaoud Region (Se Algeria). *Journal of Fundamental and Applied Sciences*, 9(1), 528.
4. Bouselsal B., Saibi H. 2022. Groundwater for Sustainable Development Evaluation of Groundwater Quality and Hydrochemical Characteristics in the Shallow Aquifer of El-Oued Region (Algerian Sahara). *Groundwater for Sustainable Development*, 17, 100747. DOI: 10.1016/j.gsd.2022.100747
5. Bouselsal B., Zouari K. 2022. Identification of Groundwater Quality and Hydrogeochemical Processes in the Shallow Aquifer of El-Oued (Algerian Sahara). *New Prospects in Environmental Geosciences and Hydrogeosciences*. Springer International Publishing. DOI: 10.1007/978-3-030-72543-3_130
6. Brown R.M., Mc Clelland N., Deininger R.A., Tozer R.G. 1970. A water quality index - do we dare. *Water Sewage Works*, 117, 339–343.
7. Busson G. 1967. *Le Mésozoïque saharien. 1ère partie : L'Extrême Sud-tunisien*. Edit., Paris, Centre Rech. Zones Arides, Géol., Ed. C.N.R.S., 8, 194.
8. Busson G. 1970. *Le Mésozoïque saharien. 2ème partie : Essai de synthèse des données des sondages algéro-tunisiens*. Edit., Paris, « Centre Rech. Zones Arides », Géol. Ed. C.N.R.S., 11, 811.
9. Castany G. 1982. Bassin sédimentaire du Sahara septentrional (Algérie-Tunisie). *Aquifère du Continental Intercalaire et du Complexe terminal*. Bull. BRGM 2 III, (2), 127–147.
10. Chadha D.K. 1999. A proposed new diagram for

- geochemical classification of natural waters and interpretation of chemical data. *Hydrogeol J.*, 7, 431–439.
11. Cornet A. 1964. Introduction à l'hydrogéologie Saharienne. *Revue de Géographie Physique et de Géologie Dynamique*, 61, 5–72.
 12. Doneen L.D. 1964. Notes on water quality in Agriculture Published as a Water Science and Engineering Paper 4001, Department of Water Science and Engineering, University of California.
 13. Freeze R.A., Cherry J.A. 1979. *Groundwater*. Printice-Hall, New Jersey.
 14. Gaillardet J., Dupre B., Louvat P., Allegre C.J. 1999. Global silicate weathering and CO₂ consumption rates deduced from the chemistry of large rivers. *Chem Geol*, 59, 3–30.
 15. Handa B.K. 1969. Description and Classification of Media for Hydrogeochemical Investigation. Symposium on Groundwater Studies in Arid and Semi-arid Regions.
 16. Jia H., Hui Q., Le Z., Wenwen F., Haike W., Yanyan G. 2020. Alterations to Groundwater Chemistry Due to Modern Water Transfer for Irrigation over Decades. *Science of the Total Environment*, 717, 137170. <https://doi.org/10.1016/j.scitotenv.2020.137170>
 17. JORADP (Official Journal of the Algerian Republic). 2011. Executive Decree No. 11-125 of March 22, 2011, relating to the quality of water for human consumption.
 18. Kebili M., Bouselsal B., Gouaidia L. 2021. Hydrochemical Characterization and Water Quality of the Continental Intercalare Aquifer in the Ghardaïa Region (Algerian Sahara). *Journal of Ecological Engineering*, 22(10), 152–162.
 19. Kelly W.P. 1940. Permissible composition and concentration of irrigation waters. *Proc Amer Soc Civ Engin*, 66, 607–613.
 20. Kharroubi M., Bouselsal B., Ouarekh M., Benaabidate L., Khadri R. 2022. Water Quality Assessment and Hydrogeochemical Characterization of the Ouargla Complex Terminal Aquifer (Algerian Sahara). *Arabian Journal of Geosciences*, 1–24.
 21. NOM. 2021. National Office of Meteorology of Hassi Messaud : Bulletins mensuels de relevé des paramètres climatologiques en Algérie (période 2007-2021). Office national météorologique. Algérie.
 22. ONS (National Statistics Office). 2021. Resident population by age, sex and wilaya.
 23. OSS (2003) Système aquifère du Sahara septentrional: gestion commune d'un bassin transfrontière. Rapport de synthèse. OSS. Tunisie.
 24. OSS (Observatoire Sahara et Sahel). 2010. Geo-aquifer: Amélioration de la connaissance et de la gestion concertée du système Aquifère du Sahara Septentrional (SASS) par l'utilisation des images satellitaires. Rapport de synthèse. OSS, Tunisie, 23.
 25. Qu S., Zheming S., Xiangyang L., Guangcai W., Jiaqian H. 2021. Multiple Factors Control Groundwater Chemistry and Quality of Multi-Layer Groundwater System in Northwest China Coalfield: Using Self-Organizing Maps (SOM). *Journal of Geochemical Exploration*, 227(March), 106795. DOI: 10.1016/j.gexplo.2021.106795
 26. Ouarekh M., Bouselsal B., Belksier M.S., Benaabidate L. 2021. Water quality assessment and hydrogeochemical characterization of the Complex Terminal aquifer in Souf valley, Algeria. *Arabian J. Geosci.* 14, 2239. <https://doi.org/10.1007/s12517-021-08498-x>
 27. Piper A.M. 1944. Graphical interpretation of water analysis. *Transactions of the American Geophysical Union.*, 25, 914-923.
 28. Raghunath H.M. 1987. *Groundwater*. Wiley Eastern Ltd., Delhi.
 29. Richards L.A. 1954. Diagnosis and improvement of saline alkali soils. Washington, DC: US Department of Agriculture, Handbook, 60.
 30. Satouh A., Bouselsal A., Chellat S., Benaabidate I. 2021. Determination of Groundwater Vulnerability Using the DRASTIC Method in Ouargla Shallow Aquifer (Algerian Sahara). *Journal of Ecological Engineering*, 22(6), 1–8. <https://doi.org/10.12911/22998993/137680>
 31. Sawyer G.N., McCarty, D.L. 1967. *Chemistry of sanitary engineers*. 2nd ed. New York: McGraw Hill, 518.
 32. Schoeller H. 1962. *Les Eaux Souterraines. Hydrologie dynamique et chimique, Recherche, Exploitation et évaluation des Ressources*. Paris: Masson et Cie, Éditeurs, 1962.
 33. Tiwari A.K., Kumar S.A., Kumar S.A., Singh M.P. 2017. Hydrogeochemical analysis and evaluation of surface water quality of Pratapgarh district, Uttar Pradesh, India. *Appl Water Sci.*, 7, 1609–1623. DOI: 10.1007/s13201-015-0313-z
 34. Tziritis E.P., Datta P.S., Barzegar R. 2017. Characterization and Assessment of Groundwater Resources in a Complex Hydrological Basin of Central Greece (Kopaida Basin) with the Joint Use of Hydrogeochemical Analysis, Multivariate Statistics and Stable Isotopes. *Aquatic Geochemistry*, 23(4), 271–298. <https://doi.org/10.1007/s10498-017-9322-x>
 35. UNESCO. 1972. *Etude des Ressources en Eau de Sahara Septentrional. (7 vols. et annexes)*. UNESCO, Paris.
 36. USSL (U.S. Salinity Laboratory Staff). 1954. Diagnosis and improvement of saline and alkali soils: U.S. Dept. Agric. Handbook, 60, 160.
 37. Vasanthavigar M., Srinivasamoorthy K., Vijayaragan K., Ganthi R.R., Chidambaram S., Anandhan P., Vasudevan S. 2010. Application of water quality index for groundwater quality assessment: Thirumanimuttar sub-basin Tamilnadu, India. *Environ*

- Monit Assess, 171, 595–609.
38. WHO. 2017. World health statistics 2017. Monitoring health for the SDGs, sustainable development goals. Geneva: World Health Organization; 2017. License: CC BY-NC-SA 3.0 IGO.
39. Wilcox L.V. 1948. The quality of water for irrigation use (No.1488-2016-124600).
40. Wilcox L.V. 1955. The quality of water for irrigation use. US Dept. of Agric. Tech Bull. 1962, Washington, DC
41. Wisitthammasri W., Chotpantarat S., Thitimakorn T. 2020. Multivariate Statistical Analysis of the Hydrochemical Characteristics of a Volcano Sedimentary Aquifer in Saraburi Province, Thailand. *Journal of Hydrology: Regional Studies*, 32 (October), 100745. DOI: 10.1016/j.ejrh.2020.100745